Impacts of Additional HONO Sources on Concentrations and Deposition of NO_y in the Beijing-Tianjin-Hebei Region of China

Ying Li[1], Junling An[1], Mizuo Kajino[2], Jian Li[1], Yu Qu[1]

1. State Key Laboratory of Atmospheric Boundary Layer Physics and Atmospheric Chemistry, Institute of Atmospheric Physics, Chinese Academy of Sciences, Beijing, China (liying-iap@mail.iap.ac.cn)
2. Meteorological Research Institute, 1-1 Nagamine, Tsukuba 305-0052, Japan

I. Introduction

Reactive nitrogen-containing compounds (NO_y) are involved in many important chemical processes in the atmosphere, including aerosol and ozone (O_3) formation (Kondo et al., 2008). HONO, an important component of NO_y, is a significant precursor of the hydroxyl radical (OH) that drives the formation of O_3 and fine particles ($PM_{2.5}$). Unknown HONO sources and their potential impacts on air quality have gained extensive interests (Li et al., 2015a and references therein) but to our current knowledge, the impact of HONO sources on regional-scale deposition of individual NO_y species has not been quantified up to date. In this study, we will evaluate the effects of three additional HONO sources on concentrations and deposition of individual NO_y species as well as the NO_y budget over the Beijing-Tianjin-Hebei (BTH) region of China during summer and winter periods of 2007.

II. HONO parameterization

Considered are the three additional HONO sources:

(1) $NO_2^*+H_2O \rightarrow HONO+OH$ ***(the NO_2^* chemistry)***, the rate constant is estimated as 9.1×10^{-14} cm^3 $molecule^{-1}$ s^{-1} (Li et al., 2008).

(2) $2NO_2+H_2O \rightarrow HONO+HNO_3$ ***(the Het)***, the rate constant is given by Jacob (2000):

$$k=\left(\frac{r_p}{D_g}+\frac{4}{u\gamma}\right)^{-1} S_a$$

k: first-order rate constant r_p: particle radius
D_g: diffusion coefficient as 10^{-5} m^2 s^{-1}
γ: uptake coefficient as 10^{-4}
u: mean molecular speed
S_a: aerosol surface area per unit volume of air

(3) HONO emissions ***(the Emis)*** included direct emissions estimated as 0.8% of NO_x emissions and 2.3% of the NO_x emitted in diesel exhaust converted to HONO via heterogeneous reaction with semi-volatile organics. $HONO/NO_x$ is ~1.18% in Beijing (Li et al., 2011).

III. Model set-up and observation data

The Weather Research and Forecasting/Chemistry (WRF-Chem) model Version 3.2.1 with the CBM-Z gas phase chemical mechanism and the MOSAIC aerosol module was chosen. Three nested domains are employed with Domain 3 covering the BTH region (Fig. 1).

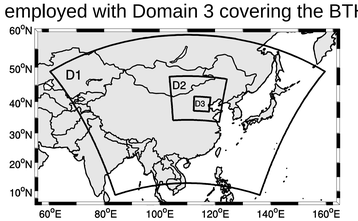

Figure 1: Modeling domains.

Measurements of NO_x, peroxyacyl nitrates (PAN), HONO, HNO_3, NO_3^-, and total gas-phase NO_y (NO_{yg}) were conducted at Peking University as part of the Campaign of Air Quality Research in Beijing (CAREBeijing-2007, Liu et al., 2010).

Table 1: Design of WRF-Chem simulations.

Case ID	HONO sources included in the WRF-Chem simulations
Case R	Reference case with HONO gas-phase production from OH and NO
Case NO_2^*	Case R + NO_2^* chemistry
Case Het	Case R + NO_2 heterogeneous reaction on aerosol surfaces
Case Emis	Case R + HONO emissions
Case E	Enhanced case with all the three additional HONO sources

Acknowledgements: The research was supported by the Beijing Municipal Natural Science Foundation (Grant No. 8144054).

IV. Impacts on concentrations of NO_y species

The updated WRF-Chem can generally well reproduce variations and quantities of the individual NO_y species, except for PAN. PAN observations were underestimated by more than 80% in both Cases R and E (Fig. 2f) due mainly to the underestimation of concentrations of acetaldehyde and methylglyoxal (Li et al., 2015b).

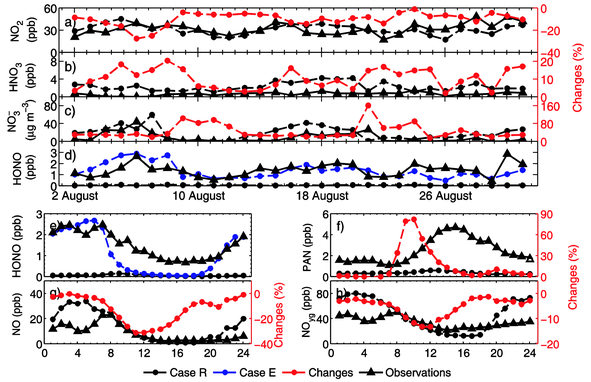

Figure 2: Comparison of observed and simulated (a-d) 24-h averages of NO_2, HNO_3, NO_3^- and HONO during 2~31 August 2007 and (e-h) diurnal averages of HONO, PAN, NO and NO_{yg} during 10~30 August 2007. Observations at Peking University in Beijing were from Liu et al. (2010). The relative concentration changes due to the three additional HONO sources are also shown in red lines.

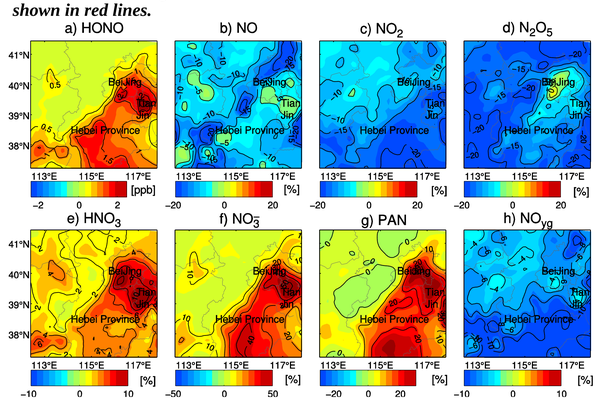

Figure 3: Monthly-mean concentration changes of (a) HONO, (b) NO, (c) NO_2, (d) N_2O_5, (e) HNO_3, (f) NO_3^-, (g) PAN, and (h) NO_{yg} over the BTH in August 2007 due to the additional HONO sources (Case E).

The additional HONO sources decreased NO_x concentrations while increased HONO, HNO_3, NO_3^-, and PAN. Overall, NO_{yg} concentrations are decreased by 6%–10% in large areas (Fig. 3). The NO_2 heterogeneous reaction is the largest contributor to the concentration changes of NO_y. The impacts of the additional HONO sources on NO_y concentrations are larger in winter than in summer (Li et al., 2015b). The concentration changes of the individual NO_y species (Fig. 3) are partially because of the OH enhancements due to the additional HONO sources (Fig. 4).

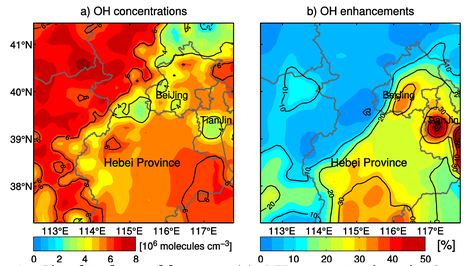

Figure 4: Simulated monthly-mean (a) OH concentrations in Case R and (b) OH enhancements due to the additional HONO sources (Case E) in August 2007.

V. Impacts on dry deposition of NO_y species

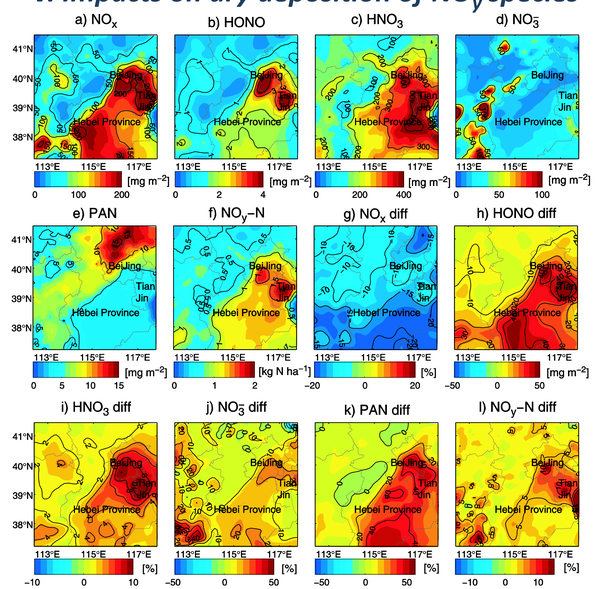

Figure 5: Simulated (a~f) dry deposition of NO_x, HONO, HNO_3, NO_3^-, PAN, and the total N in NO_y in August 2007 from the reference run (Case R) and (g~l) percentage changes due to the additional HONO sources (Case E).

The additional HONO sources decreased NO_x dry deposition while increased dry deposition of HONO, HNO_3, NO_3^-, PAN and the total N in NO_y (NO_y-N) (Fig. 5). Changes in the dry deposition of NO_y species correspond to their concentration changes (Fig. 3). The dominant contributor to the changes of NO_y dry deposition is the NO_2 heterogeneous reaction. The impact on NO_y dry deposition in winter is larger than that in summer (Li et al., 2015b).

References:

Kondo, Y. and co-authors (2008) *J. Geophys. Res.*, **113**, doi: 10.1029/2008JD010134.

Li, S. and co-authors (2008) *Science*, **319**, 1657-1660.

Li, Y. and co-authors (2011) *Atmos. Environ.*, **45**, 4735-4744.

Li, Y. and co-authors (2015a) *Tellus B*, **67**, 23930, http://dx.doi.org/10.3402/tellusb.v67.23930.

Li, Y. and co-authors (2015b) *SOLA*, **11**, 36-42.

Liu, Z. and co-authors (2010) *Environ. Sci. Technol.*, **44**, 7017-7022.

VI. Impacts on NO_3^- wet deposition

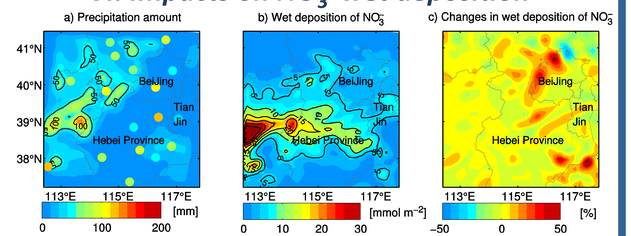

Figure 6: Simulated (a) precipitation amount and (b) wet deposition amount of nitrate in August 2007 from the reference run (Case R) and (c) percentage changes due to the additional HONO sources (Case E). Observations of the precipitation amount at seventeen meteorological stations over the BTH region are indicated by colored dots.

Wet deposition of NO_3^- (W-NO_3^-) was found with ~20% increases in a few areas of the BTH in August (Fig. 6).

VII. Impacts on the NO_y budget

Species	Case R	Case NO_2^*	Case Het	Case Emis	Case E
August 2007					
Dry deposition amount over the BTH region					
NO	0.49	(-11.0)	(-53.2)	(-3.4)	0.46 (-57.8)
NO_2	6.7	(1.3)	(-29.0)	(1.0)	5.7 (-30.6)
HONO	0.10	(61.3)	(2653.9)	(359.8)	1.4 (2762.3)
HNO_3	11.4	(5.9)	(10.3)	(3.4)	11.9 (15.3)
NO_3^-	1.4	(30.9)	(40.1)	(27.1)	1.6 (54.3)
PAN	0.08	(10.7)	(36.3)	(2.9)	0.09 (45.2)
Total	20.2	(4.7)	(48.2)	(13.1)	21.1 (54.3)
Wet deposition amount over the BTH region					
HNO_3	0.07	(98.5)	(190.5)	(125.3)	0.07 (205.9)
NO_3^-	16.7	(319.8)	(250.2)	(182.9)	17.2 (161.8)
Total	16.8	(309.2)	(244.2)	(180.1)	17.3 (161.3)
Total emissions over the BTH region					
NO	54.3	54.3	54.3	54.0	54.0
HONO	0	0	0	0.3	0.3
February 2007					
Dry deposition amount over the BTH region					
NO	0.08	(33.5)	(-69.5)	(25.5)	0.06 (-73.7)
NO_2	2.9	(-2.0)	(-42.8)	(-2.3)	2.3 (-46.0)
HONO	0.05	(36.5)	(4549.7)	(489.3)	1.3 (4766.5)
HNO_3	0.2	(6.4)	(62.3)	(5.6)	0.3 (73.8)
NO_3^-	0.7	(-13.5)	(110.8)	(-20.9)	0.9 (115.3)
PAN	0.08	(-16.1)	(63.2)	(-17.5)	0.1 (88.1)
Total	4.0	(3.6)	(148.6)	(14.9)	5.0 (166.0)
Wet deposition amount over the BTH region					
HNO_3	1.0×10^{-3}	(109.8)	(422.5)	(124.1)	1.0×10^{-3} (493.1)
NO_3^-	3.6	(56.8)	(165.8)	(30.1)	4.1 (173.8)
Total	3.6	(56.8)	(165.4)	(30.1)	4.1 (173.7)
Total emissions over the BTH region					
NO	54.3	54.3	54.3	54.0	54.0
HONO	0	0	0	0.3	0.3

Table 2: Regional dry and wet deposition amounts of each NO_y species (Gg N) and monthly-mean emissions of NO_x (Gg N) over the BTH region. The maximum differences of NO_y deposition amounts over the BTH between Case R and Case NO_2^*, Case Het, Case Emis, and Case E, respectively, are provided in parentheses.

The total deposition of NO_y is increased by 1.4 Gg N (1.5 Gg N) over the BTH in August (February).

VIII. Conclusions

The significant impacts of the additional HONO sources on concentrations and deposition of NO_y suggest that the additional HONO sources aggravate regional-scale acid deposition, emphasizing the importance of the additional HONO sources in the NO_y budget.